Determination of interaction forces between parallel dislocations by the evaluation of J integrals of plane elasticity

Vlado A. Lubarda

Continuum Mechanics and Thermodynamics

ISSN 0935-1175

Continuum Mech. Thermodyn.
DOI 10.1007/s00161-015-0438-1

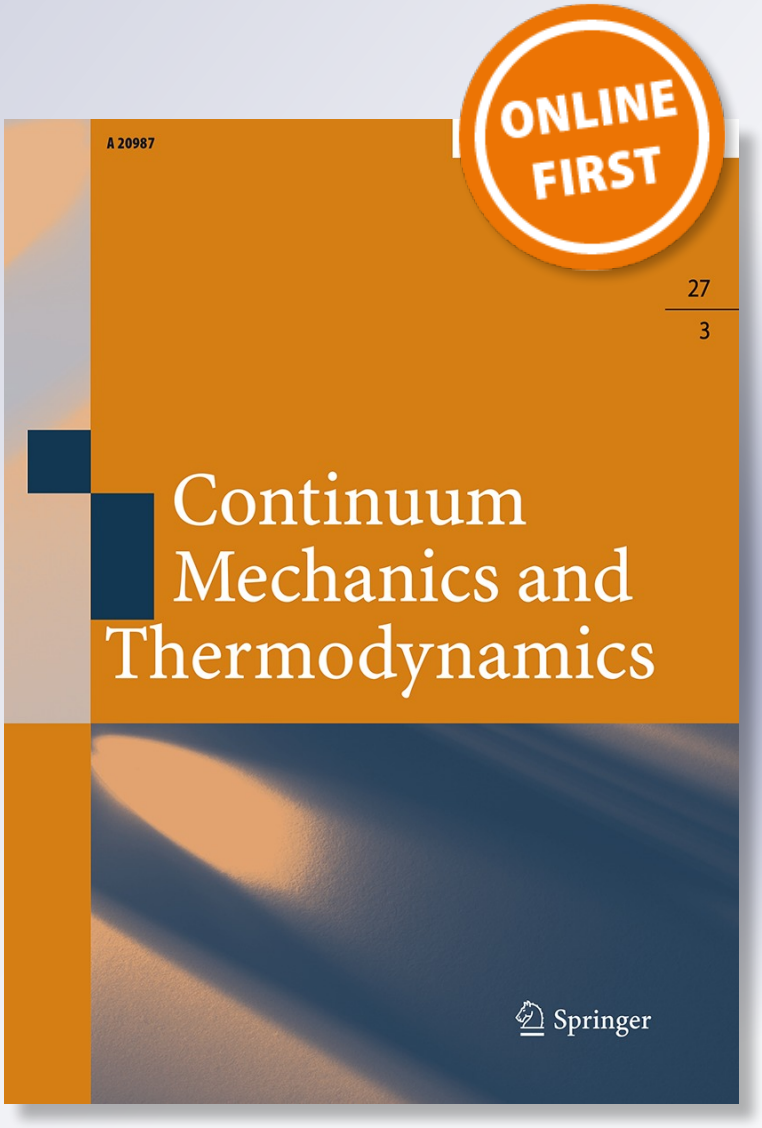

Springer

Continuum Mech. Thermodyn.
DOI 10.1007/s00161-015-0438-1

ORIGINAL ARTICLE

Vlado A. Lubarda

Determination of interaction forces between parallel dislocations by the evaluation of J integrals of plane elasticity

Received: 6 October 2014 / Accepted: 4 May 2015

Abstract The Peach–Koehler expressions for the glide and climb components of the force exerted on a straight dislocation in an infinite isotropic medium by another straight dislocation are derived by evaluating the plane and antiplane strain versions of J integrals around the center of the dislocation. After expressing the elastic fields as the sums of elastic fields of each dislocation, the energy momentum tensor is decomposed into three parts. It is shown that only one part, involving mixed products from the two dislocation fields, makes a nonvanishing contribution to J integrals and the corresponding dislocation forces. Three examples are considered, with dislocations on parallel or intersecting slip planes. For two edge dislocations on orthogonal slip planes, there are two equilibrium configurations in which the glide and climb components of the dislocation force simultaneously vanish. The interactions between two different types of screw dislocations and a nearby circular void, as well as between parallel line forces in an infinite or semi-infinite medium, are then evaluated.

Keywords Climb force · Dislocation · Energy momentum tensor · Glide force · J integral · Line force · Peach–Koehler force · Strain energy · Void

1 Introduction

In the wake of Eshelby's [1,2] work on the energy momentum tensor and the subsequent developments in [3–7], there have been numerous contributions to the study of conservation integrals and configurational forces on material defects, such as cracks, voids, inclusions, grain or phase boundaries, and dislocations. A comprehensive survey of the field, with the referral to the original contributions, can be found in the review papers or books [8–11]. The objective of the present paper is to derive the expressions for the components of the force exerted on a straight dislocation by another parallel straight dislocation by evaluating the two-dimensional version of J integrals around the dislocation, rather than by deducing them from the general

Communicated by Victor Eremeyev, Peter Schiavone and Francesco dell'Isola.

V. A. Lubarda (✉)
Departments of NanoEngineering and Mechanical and Aerospace Engineering,
University of California, San Diego, La Jolla, CA 92093-0448, USA
E-mail: vlubarda@ucsd.edu

V. A. Lubarda
Montenegrin Academy of Sciences and Arts, Rista Stijovića 5,
81000 Podgorica, Montenegro

Published online: 13 May 2015

Peach–Koehler expression for the dislocation force $\mathbf{F} = (\boldsymbol{\sigma} \cdot \mathbf{b}) \times \mathbf{e}_3$.[1] If the Burgers vector of the straight dislocation along the $\mathbf{e}_3$ direction is $\mathbf{b} = \{b_1, b_2, b_3\}$ and if $\boldsymbol{\sigma}$ is the stress tensor along the dislocation line produced by the second dislocation, the components of the dislocation force (per unit dislocation length) are

$$F_1 = \sigma_{21}b_1 + \sigma_{22}b_2 + \sigma_{23}b_3, \quad F_2 = -(\sigma_{11}b_1 + \sigma_{12}b_2 + \sigma_{13}b_3). \tag{1}$$

The derivation of these expressions by the J integrals evaluation is tedious, if the integrals are evaluated using the total stress and displacement fields, as done, for example, in [16]. The calculations are, however, significantly simplified if the elastic fields are decomposed into the sums of the elastic fields of each dislocation alone. This gives rise to the decomposition of the energy momentum tensor into three parts. It is shown in Sect. 2 that only one part of the energy momentum tensor, involving mixed products of two dislocation fields, contributes to the J integrals and the corresponding dislocation forces.[2] Since there is no interaction between parallel edge and screw dislocations, the interaction forces are first evaluated between two edge dislocations (Sects. 3, 4), and then between two screw dislocations (Sect. 5). The forces between mixed-type parallel dislocations are obtained by superposition (Sect. 6). Three examples are considered to illustrate the application of the derived formulas. These include two edge dislocations on parallel and orthogonal slip planes (Sect. 4), and two mixed-type straight dislocations on intersecting slip planes (Sect. 6). Interaction forces between different types of screw dislocations and a nearby circular void are deduced from the expressions for the interaction forces between two or three screw dislocations in an infinite medium (Sect. 7). The interaction between parallel line forces in an infinite and semi-infinite medium under antiplane strain conditions is evaluated in Sect. 8. Concluding remarks with discussion are given in Sect. 9.

2 Decomposition of the energy momentum tensor

The J integrals of the plane strain infinitesimal elastic deformations are

$$J_\beta = \oint P_{\alpha\beta} n_\alpha \, \mathrm{d}l, \quad (\alpha, \beta) = 1, 2, \tag{2}$$

evaluated over a closed contour whose infinitesimal element is $\mathrm{d}l$ with the outward normal n_α. The components of the energy momentum tensor $P_{\alpha\beta}$ [2] are defined by

$$P_{\alpha\beta} = W\delta_{\alpha\beta} - \sigma_{\alpha\gamma}u_{\gamma,\beta}, \quad W = \frac{1}{2}\sigma_{\alpha\beta}\epsilon_{\alpha\beta}. \tag{3}$$

The strain energy density is denoted by W. The inplane strain components are related to stress components by Hooke's law

$$\epsilon_{\alpha\beta} = \frac{1}{2\mu}\left(\sigma_{\alpha\beta} - \nu\sigma_{\gamma\gamma}\delta_{\alpha\beta}\right), \tag{4}$$

where μ is the elastic shear modulus, ν is the Poisson ratio, and $\sigma_{\gamma\gamma} = \sigma_{11} + \sigma_{22}$.

Two edge dislocations parallel to the x_3 direction, at the distance d from each other, are shown in Fig. 1. Their Burgers vectors have the magnitudes b' and b'', with the orientation φ' and φ'' relative to the x_1 axis. The objective is to determine the components of the interaction forces between these dislocations (Fig. 2). The total elastic stress, strain, and displacement fields can be expressed as the sum of the elastic fields from each dislocation alone, i.e.,

$$\sigma_{\alpha\beta} = \sigma'_{\alpha\beta} + \sigma''_{\alpha\beta}, \quad \epsilon_{\alpha\beta} = \epsilon'_{\alpha\beta} + \epsilon''_{\alpha\beta}, \quad u_{\alpha,\beta} = u'_{\alpha,\beta} + u''_{\alpha,\beta}. \tag{5}$$

Upon the substitution of (5) into (3), the strain energy and the components of the energy momentum tensor are found to be

$$W = W' + W'' + \sigma'_{\alpha\beta}\epsilon''_{\alpha\beta}, \tag{6}$$

$$P_{\alpha\beta} = P'_{\alpha\beta} + P''_{\alpha\beta} + \hat{P}_{\alpha\beta}, \tag{7}$$

[1] Peach and Koehler [12] derived a general expression for the force on a line element of a curved dislocation in an arbitrary stress field by applying the energy/work analysis associated with an infinitesimal translation of a dislocation loop. See also the energy analysis in [13–15].

[2] To evaluate configurational forces in a more general setting, with arbitrary external or image loading, or arbitrary sources of internal stress, Eshelby [1,2] also used the decomposition of the elastic fields into their constituent parts.

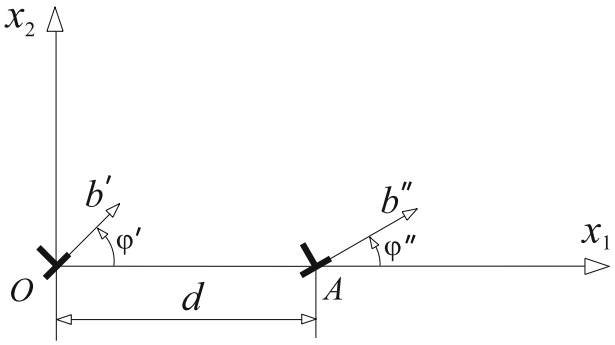

Fig. 1 Two edge dislocations with the Burgers vectors b' and b'', whose angles of orientation relative to the x_1 axis are φ' and φ''. The normal distance between two dislocations is d

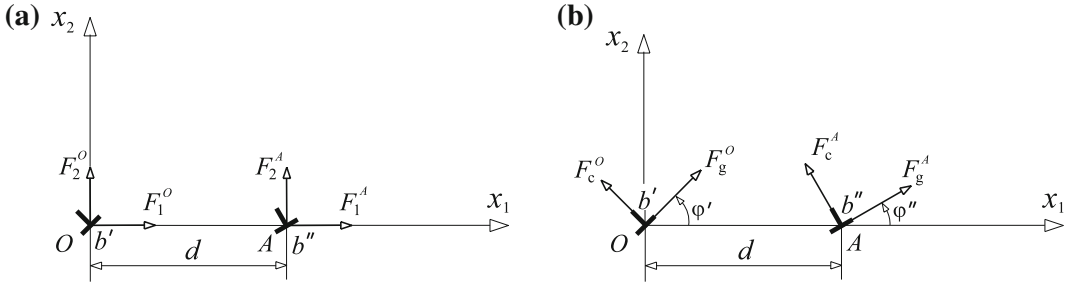

Fig. 2 **a** x_1 and x_2 components of the dislocation forces at O and A. Two sets of components are related by $F_1^A = -F_1^O$ and $F_2^A = -F_2^0$. **b** The glide and climb components of the forces on two dislocations

where

$$W' = \frac{1}{2}\sigma'_{\alpha\beta}\epsilon'_{\alpha\beta}, \quad W'' = \frac{1}{2}\sigma''_{\alpha\beta}\epsilon''_{\alpha\beta}, \tag{8}$$

and

$$P'_{\alpha\beta} = W'\delta_{\alpha\beta} - \sigma'_{\alpha\gamma}u'_{\gamma,\beta}, \quad P''_{\alpha\beta} = W''\delta_{\alpha\beta} - \sigma''_{\alpha\gamma}u''_{\gamma,\beta}. \tag{9}$$

The remaining part of the energy momentum tensor in (7) is a mixed or coupling part[3]

$$\hat{P}_{\alpha\beta} = \sigma'_{mn}\epsilon''_{mn}\delta_{\alpha\beta} - \left(\sigma'_{\alpha\gamma}u''_{\gamma,\beta} + \sigma''_{\alpha\gamma}u'_{\gamma,\beta}\right). \tag{10}$$

In view of the Hooke's law (4), the trace term in (10) can be rewritten as

$$\sigma'_{mn}\epsilon''_{mn} = \frac{1}{2\mu}\left(\sigma'_{mn}\sigma''_{mn} - \nu\sigma'_{mm}\sigma''_{nn}\right), \tag{11}$$

so that (10) becomes

$$\hat{P}_{\alpha\beta} = \frac{1}{2\mu}\left(\sigma'_{mn}\sigma''_{mn} - \nu\sigma'_{mm}\sigma''_{nn}\right)\delta_{\alpha\beta} - \left(\sigma'_{\alpha\gamma}u''_{\gamma,\beta} + \sigma''_{\alpha\gamma}u'_{\gamma,\beta}\right). \tag{12}$$

Explicitly, the four components of the mixed part of the energy momentum tensor $\hat{P}_{\alpha\beta}$ are

[3] This can be compared with the Eshelby's analysis of cross-terms appearing in the expression for the force on an elastic singularity [2, p. 104].

$$\begin{aligned}
\hat{P}_{11} &= \frac{1}{2\mu}\left[\left(\sigma''_{11}\sigma'_{11}+\sigma''_{22}\sigma'_{22}+2\sigma''_{12}\sigma'_{12}\right)-\nu\left(\sigma''_{11}+\sigma''_{22}\right)\left(\sigma'_{11}+\sigma'_{22}\right)\right]\\
&\quad-\left(u''_{1,1}\sigma'_{11}+u''_{2,1}\sigma'_{12}+\sigma''_{11}u'_{1,1}+\sigma''_{12}u'_{2,1}\right),\\
\hat{P}_{22} &= \frac{1}{2\mu}\left[\left(\sigma''_{11}\sigma'_{11}+\sigma''_{22}\sigma'_{22}+2\sigma''_{12}\sigma'_{12}\right)-\nu\left(\sigma''_{11}+\sigma''_{22}\right)\left(\sigma'_{11}+\sigma'_{22}\right)\right]\\
&\quad-\left(u''_{1,2}\sigma'_{21}+u''_{2,2}\sigma'_{22}+\sigma''_{21}u'_{1,2}+\sigma''_{22}u'_{2,2}\right),\\
\hat{P}_{12} &= -\left(u''_{1,2}\sigma'_{11}+u''_{2,2}\sigma'_{12}+\sigma''_{11}u'_{1,2}+\sigma''_{12}u'_{2,2}\right),\\
\hat{P}_{21} &= -\left(u''_{1,1}\sigma'_{21}+u''_{2,1}\sigma'_{22}+\sigma''_{21}u'_{1,1}+\sigma''_{22}u'_{2,1}\right).
\end{aligned} \tag{13}$$

2.1 **J** integrals around the dislocation

Upon the substitution of (7) into (2), the J_β integrals can be additively decomposed as

$$J_\beta = J'_\beta + J''_\beta + \hat{J}_\beta, \tag{14}$$

where

$$J'_\beta = \oint P'_{\alpha\beta}n_\alpha \,\mathrm{d}l, \quad J''_\beta = \oint P''_{\alpha\beta}n_\alpha \,\mathrm{d}l, \quad \hat{J}_\beta = \oint \hat{P}_{\alpha\beta}n_\alpha \,\mathrm{d}l. \tag{15}$$

To evaluate the configurational forces on the dislocation with its center at point O, exerted by the dislocation with its center at point A, the J_β integrals are evaluated around a small circle of radius r about the center of the dislocation at O. The J'_β integrals in (15) vanish because the dislocation alone in an infinite medium does not exert any force on itself. The J''_β integrals also vanish, because the elastic fields $''$ from the dislocation at A are non-singular within a small circle around the core of the dislocation at O. Thus, $J'_\beta = 0$, $J''_\beta = 0$, and (14) reduces to

$$J_\beta = \hat{J}_\beta = \oint \hat{P}_{\alpha\beta}n_\alpha \,\mathrm{d}l. \tag{16}$$

Its component representation is

$$J_1 = \int_0^{2\pi}\left(\hat{P}_{11}\cos\theta + \hat{P}_{21}\sin\theta\right) r\,\mathrm{d}\theta, \quad J_2 = \int_0^{2\pi}\left(\hat{P}_{12}\cos\theta + \hat{P}_{22}\sin\theta\right) r\,\mathrm{d}\theta. \tag{17}$$

3 Dislocation stress and displacement fields

The stress components due to edge dislocation with the Burgers vector $\mathbf{b} = \{b_1, b_2, 0\}$ in an infinite isotropic medium are [17]

$$\begin{aligned}
\sigma_{11} &= -kb_1x_2\,\frac{3x_1^2+x_2^2}{r^4} + kb_2x_1\,\frac{x_1^2-x_2^2}{r^4},\\
\sigma_{22} &= kb_2x_1\,\frac{x_1^2+3x_2^2}{r^4} + kb_1x_2\,\frac{x_1^2-x_2^2}{r^4},\\
\sigma_{12} &= kb_1x_1\,\frac{x_1^2-x_2^2}{r^4} + kb_2x_2\,\frac{x_1^2-x_2^2}{r^4},
\end{aligned} \tag{18}$$

where

$$k = \frac{\mu}{2\pi(1-\nu)}. \tag{19}$$

The corresponding displacement components, to within an arbitrary constant, are

$$\begin{aligned}
u_1 &= \frac{b_1}{2\pi}\left[\tan^{-1}\frac{x_2}{x_1} + \frac{1}{2(1-\nu)}\,\frac{x_1x_2}{r^2}\right] + \frac{b_2}{8\pi(1-\nu)}\left[(1-2\nu)\ln r^2 - \frac{x_1^2-x_2^2}{r^2}\right],\\
u_2 &= \frac{b_2}{2\pi}\left[\tan^{-1}\frac{x_2}{x_1} - \frac{1}{2(1-\nu)}\,\frac{x_1x_2}{r^2}\right] - \frac{b_1}{8\pi(1-\nu)}\left[(1-2\nu)\ln r^2 + \frac{x_1^2-x_2^2}{r^2}\right].
\end{aligned} \tag{20}$$

The displacement gradients, needed for the evaluation of the components of the energy momentum tensor listed in (13), are

$$
\begin{aligned}
u_{1,1} &= -\frac{b_1}{2\pi}\left[\frac{x_2}{r^2}+\frac{1}{2(1-\nu)}\,\frac{x_2(x_1^2-x_2^2)}{r^4}\right]+\frac{b_2}{4\pi(1-\nu)}\left[(1-2\nu)\,\frac{x_1}{r^2}-\frac{2x_1x_2^2}{r^4}\right],\\
u_{2,2} &= \frac{b_2}{2\pi}\left[\frac{x_1}{r^2}-\frac{1}{2(1-\nu)}\,\frac{x_1(x_1^2-x_2^2)}{r^4}\right]-\frac{b_1}{4\pi(1-\nu)}\left[(1-2\nu)\,\frac{x_2}{r^2}-\frac{2x_1^2x_2}{r^4}\right],\\
u_{1,2} &= \frac{b_1}{2\pi}\left[\frac{x_1}{r^2}+\frac{1}{2(1-\nu)}\,\frac{x_1(x_1^2-x_2^2)}{r^4}\right]+\frac{b_2}{4\pi(1-\nu)}\left[(1-2\nu)\,\frac{x_2}{r^2}+\frac{2x_1^2x_2}{r^4}\right],\\
u_{2,1} &= -\frac{b_2}{2\pi}\left[\frac{x_2}{r^2}-\frac{1}{2(1-\nu)}\,\frac{x_2(x_1^2-x_2^2)}{r^4}\right]-\frac{b_1}{4\pi(1-\nu)}\left[(1-2\nu)\,\frac{x_1}{r^2}+\frac{2x_1x_2^2}{r^4}\right].
\end{aligned}
\tag{21}
$$

3.1 Elastic fields along a small circle around dislocation $\mathbf{b}'$

Along a small circle of radius r around the dislocation at O, the stress components from the dislocation itself are obtained from (18) by taking $x_1 = rc$ and $x_2 = rs$, where $c = \cos\theta$ and $s = \sin\theta$. This gives

$$
\begin{aligned}
r\sigma'_{11} &= -kb'_1 s\left(3c^2+s^2\right)+kb'_2 c\left(c^2-s^2\right),\\
r\sigma'_{22} &= kb'_2 c\left(3s^2+c^2\right)+kb'_1 s\left(c^2-s^2\right),\\
r\sigma'_{12} &= kb'_1 c\left(c^2-s^2\right)+kb'_2 s\left(c^2-s^2\right).
\end{aligned}
\tag{22}
$$

Similarly, from (21), the displacement gradients along a small circle around O are

$$
\begin{aligned}
ru'_{1,1} &= -\frac{b'_1}{2\pi}\left[s+\frac{1}{2(1-\nu)}\,s(c^2-s^2)\right]+\frac{b'_2}{4\pi(1-\nu)}\left[(1-2\nu)c-2cs^2\right],\\
ru'_{2,2} &= \frac{b'_2}{2\pi}\left[c-\frac{1}{2(1-\nu)}\,c(c^2-s^2)\right]-\frac{b'_1}{4\pi(1-\nu)}\left[(1-2\nu)s-2c^2s\right],\\
ru'_{1,2} &= \frac{b'_1}{2\pi}\left[c+\frac{1}{2(1-\nu)}\,c(c^2-s^2)\right]+\frac{b'_2}{4\pi(1-\nu)}\left[(1-2\nu)s+2c^2s\right],\\
ru'_{2,1} &= -\frac{b'_2}{2\pi}\left[s-\frac{1}{2(1-\nu)}\,s(c^2-s^2)\right]-\frac{b'_1}{4\pi(1-\nu)}\left[(1-2\nu)c+2cs^2\right].
\end{aligned}
\tag{23}
$$

If the radius of a small circle around the dislocation at O is much smaller than the distance from O to A ($r \ll d$), the elastic fields along the small circle around O due to dislocation b'' are obtained from (18) and (21) by substituting $x_1 \approx -d$ and $x_2 \approx 0$. This gives the non-singular fields

$$
\sigma''_{11} = \sigma''_{22} = -k\,\frac{b''_2}{d}, \quad \sigma''_{12} = \sigma''_{21} = -k\,\frac{b''_1}{d},
\tag{24}
$$

and

$$
\begin{aligned}
u''_{1,1} &= -\frac{1-2\nu}{4\pi(1-\nu)}\,\frac{b''_2}{d} = \frac{1-2\nu}{2\mu}\,\sigma''_{11}, \quad u''_{2,2} = -\frac{1-2\nu}{4\pi(1-\nu)}\,\frac{b''_2}{d} = \frac{1-2\nu}{2\mu}\,\sigma''_{22},\\
u''_{1,2} &= -\frac{3-2\nu}{4\pi(1-\nu)}\,\frac{b''_1}{d} = \frac{3-2\nu}{2\mu}\,\sigma''_{12}, \quad u''_{2,1} = \frac{1-2\nu}{4\pi(1-\nu)}\,\frac{b''_1}{d} = -\frac{1-2\nu}{2\mu}\,\sigma''_{21}.
\end{aligned}
\tag{25}
$$

4 Configurational forces between two edge dislocations

The substitution of (22)–(25) into (17), followed by a straightforward integration, yields

$$J_1^O = \sigma''_{21} b'_1 + \sigma''_{22} b'_2, \quad J_2^O = -\left(\sigma''_{11} b'_1 + \sigma''_{12} b'_2\right), \tag{26}$$

which are the Peach–Koehler expressions for the force components on the edge dislocation $\mathbf{b}'$ due to edge dislocation $\mathbf{b}''$. When the stress components (24) are incorporated into (26), the horizontal and vertical components of the force on the dislocation at O (Fig. 2a) become

$$F_1^O = J_1^O = -\frac{k}{d}\left(b'_1 b''_1 + b'_2 b''_2\right), \quad F_2^O = J_2^O = \frac{k}{d}\left(b'_1 b''_2 + b''_1 b'_2\right). \tag{27}$$

In terms of the magnitudes of the Burgers vectors (b' and b'') and their orientations (φ' and φ''), (27) can be rewritten as

$$F_1^O = -\frac{kb'b''}{d}\cos(\varphi' - \varphi''), \quad F_2^O = \frac{kb'b''}{d}\sin(\varphi' + \varphi''). \tag{28}$$

The corresponding glide and climb components of the force (Fig. 2b) are

$$F_{\mathrm{g}}^O = F_1^O \cos\varphi' + F_2^O \sin\varphi', \quad F_{\mathrm{c}}^O = F_2^O \cos\varphi' - F_1^O \sin\varphi', \tag{29}$$

i.e., after the substitution of (28),

$$F_{\mathrm{g}}^O = -\frac{kb'b''}{d}\cos\varphi'' \cos 2\varphi', \quad F_{\mathrm{c}}^O = \frac{kb'b''}{d}(\sin\varphi'' + \cos\varphi'' \sin 2\varphi'). \tag{30}$$

Since $J_\beta^O + J_\beta^A = 0$ for each β (because the translation of both dislocations together does not change the strain energy in an infinite medium), we have $F_1^A = -F_1^O$ and $F_2^A = -F_2^O$. Thus, from (27) and

$$F_{\mathrm{g}}^A = -F_1^O \cos\varphi'' - F_2^O \sin\varphi'', \quad F_{\mathrm{c}}^A = -F_2^O \cos\varphi'' + F_1^O \sin\varphi'', \tag{31}$$

the glide and climb components of the force on the dislocation at A are

$$F_{\mathrm{g}}^A = \frac{kb'b''}{d}\cos\varphi' \cos 2\varphi'', \quad F_{\mathrm{c}}^A = -\frac{kb'b''}{d}(\sin\varphi' + \cos\varphi' \sin 2\varphi''). \tag{32}$$

4.1 Examples

Expressions (31) and (32) are the general expressions for the forces between two edge dislocations, from which some well-known cases follow directly. For example, two edge dislocations on two parallel slip planes, the distance $h = d\sin\alpha$ apart from each other, are shown in Fig. 3a. The product of the dislocation Burgers vectors is $b'b'' = b^2 \mathrm{sign}(b'b'')$, where b is the magnitude of the Burgers vector of each dislocation. The glide and climb forces on the dislocation at A are obtained from (32) by taking $\varphi' = \varphi'' = -\alpha$, which gives

$$F_{\mathrm{g}}^A = \frac{kb'b''}{d}\cos\alpha\cos 2\alpha, \quad F_{\mathrm{c}}^A = \frac{kb'b''}{d}\sin\alpha(2 + \cos 2\alpha). \tag{33}$$

The variations of the glide and climb forces with the angle $\alpha \in [0, 180°]$, keeping the distance d between two dislocations fixed, are shown in Fig. 4a. The maximum climb force occurs at $\alpha = 45°$ and $\alpha = 135°$ and is equal to $\sqrt{2}$ times the maximum magnitude of the glide force ($kb'b''/d$), which occurs at $\alpha = 0°$ and $\alpha = 180°$. When rewritten in terms of $a = d\cos\alpha$ and $h = d\sin\alpha$, the expressions (33) take the well-known form [17,18]

$$F_{\mathrm{g}}^A = kb'b''\frac{a(a^2 - h^2)}{(a^2 + h^2)^2}, \quad F_{\mathrm{c}}^A = kb'b''\frac{h(3a^2 + h^2)}{(a^2 + h^2)^2}. \tag{34}$$

The variations of these forces with the horizontal distance a, at fixed h, are shown in Fig. 5a. The maximum climb force $F_{\mathrm{c}}^{\max} = (9/8)kb'b''/h$ occurs at $a = \sqrt{3}h/3$ and is 4.5 times greater than the magnitude of the maximum glide force $F_{\mathrm{g}}^{\max} = (1/4)kb'b''/h$, which occurs at $a = \pm\sqrt{2}h$ and $a = (-1 \pm \sqrt{2})h$. The

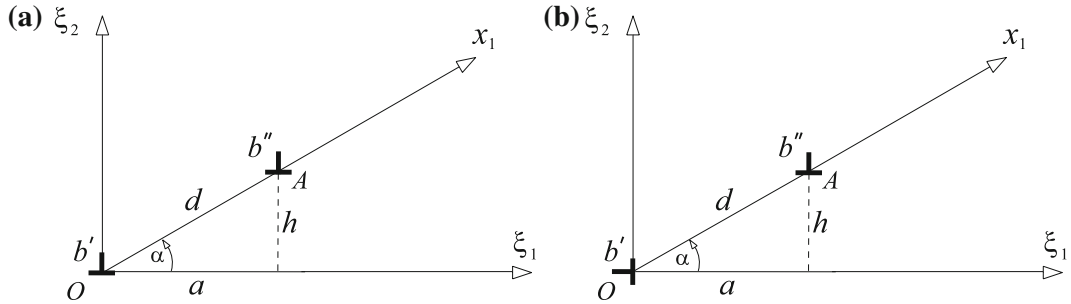

Fig. 3 **a** Two edge dislocations (b' and b'') on parallel slip planes, a distance h apart from each other. **b** Two edge dislocations on orthogonal slip planes

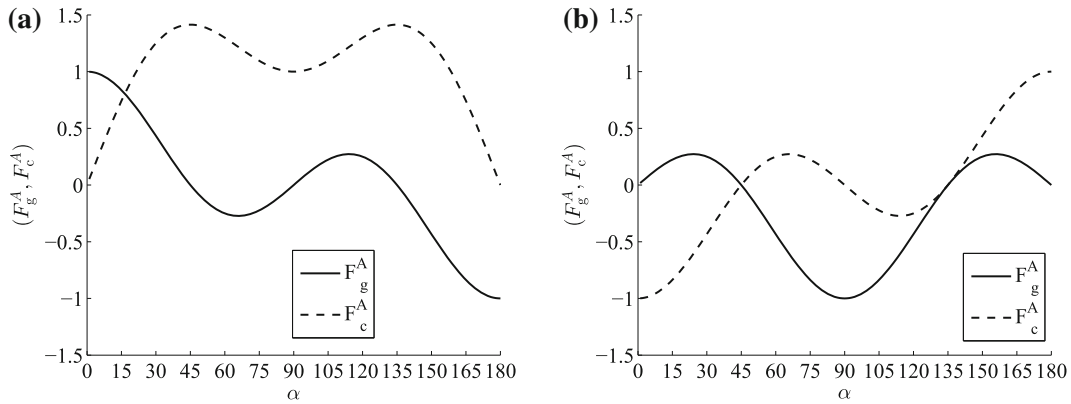

Fig. 4 **a** Variations of the glide and climb forces on the dislocation at A (Fig. 3a) with the angle α, at fixed distance d. The forces are scaled by $kb'b''/d$. **b** The same as in **a**, but for dislocations on orthogonal slip planes, shown in Fig. 3b

glide force vanishes at $a = 0$ and $a = \pm h$. The corresponding climb force at all three of these locations is $F_c = kb'b''/h$.

If two edge dislocations are on orthogonal slip planes (Fig. 3b), then

$$F_g^A = -\frac{kb'b''}{d}\cos\alpha\cos 2\alpha, \quad F_c^A = -\frac{kb'b''}{d}\sin\alpha\cos 2\alpha. \tag{35}$$

The variations of the corresponding glide and climb forces acting on the dislocation at A with the angle α are shown in Fig. 4b. The glide and climb forces both vanish at $\alpha = 45°$ and $\alpha = 135°$. When rewritten in terms of a and h, (35) becomes

$$F_g^A = kb'b''\frac{h(a^2-h^2)}{(a^2+h^2)^2}, \quad F_c^A = -kb'b''\frac{a(a^2-h^2)}{(a^2+h^2)^2}. \tag{36}$$

Their variations with the horizontal distance a, at fixed h, are shown in Fig. 5b. The maximum magnitude of the glide force $F_g^{\max} = kb'b''/h$ occurs at $a = 0$ and is 4 times greater than the maximum magnitude of the climb force $F_c^{\max} = (1/4)kb'b''/h$, which occurs at $a = \pm\sqrt{2}h$ and $a = (-1 \pm \sqrt{2})h$. The glide and climb forces simultaneously vanish at $a = \pm h$, so that two dislocations in these positions are in equilibrium with respect to both glide and climb.

5 Interaction between two screw dislocations

The J integrals of the antiplane strain elasticity are defined by (2), with the energy momentum tensor given by

$$P_{\alpha\beta} = W\delta_{\alpha\beta} - \sigma_{3\alpha}u_{3,\beta} = W\delta_{\alpha\beta} - \frac{1}{\mu}\sigma_{3\alpha}\sigma_{3\beta}, \quad W = \frac{1}{2\mu}\sigma_{3\gamma}\sigma_{3\gamma}, \tag{37}$$

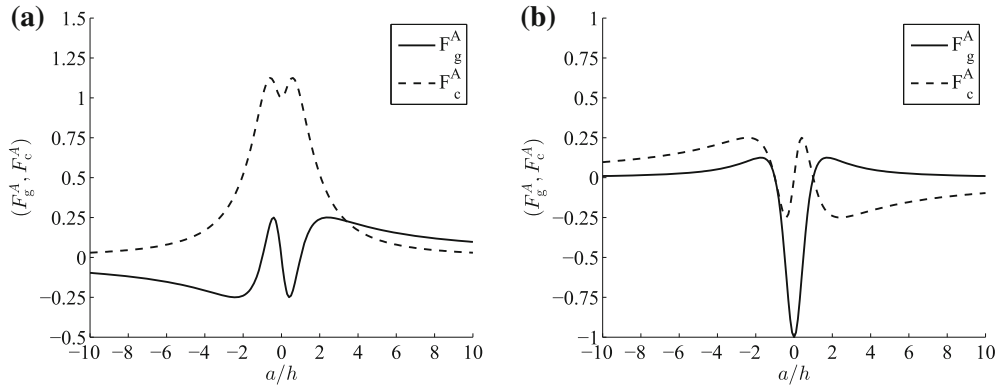

Fig. 5 **a** Variation of the glide and climb forces on the dislocation at A (Fig. 3a) with the horizontal distance a, at fixed h. The forces are scaled by $kb'b''/h$. **b** The same for the dislocations on orthogonal slip planes, shown in Fig. 3b

i.e.,

$$P_{\alpha\beta} = \frac{1}{2\mu}\,(\sigma_{3\gamma}\sigma_{3\gamma}\delta_{\alpha\beta} - 2\sigma_{3\alpha}\sigma_{3\beta}). \tag{38}$$

If the elastic stress field is expressed as the sum of the elastic fields from each dislocation alone ($\sigma_{3\alpha} = \sigma'_{3\alpha} + \sigma''_{3\alpha}$), the energy momentum tensor (38) becomes $P_{\alpha\beta} = P'_{\alpha\beta} + P''_{\alpha\beta} + \hat{P}_{\alpha\beta}$, where

$$P'_{\alpha\beta} = \frac{1}{2\mu}\left(\sigma'_{3\gamma}\sigma'_{3\gamma}\delta_{\alpha\beta} - 2\sigma'_{3\alpha}\sigma'_{3\beta}\right), \quad P''_{\alpha\beta} = \frac{1}{2\mu}\left(\sigma''_{3\gamma}\sigma''_{3\gamma}\delta_{\alpha\beta} - 2\sigma''_{3\alpha}\sigma''_{3\beta}\right). \tag{39}$$

The remaining coupling part of the energy momentum tensor is

$$\hat{P}_{\alpha\beta} = \frac{1}{\mu}\left(\sigma'_{3\gamma}\sigma''_{3\gamma}\delta_{\alpha\beta} - \sigma'_{3\alpha}\sigma''_{3\beta} - \sigma''_{3\alpha}\sigma'_{3\beta}\right), \tag{40}$$

which is a symmetric deviatoric two-dimensional tensor ($\hat{P}_{12} = \hat{P}_{21}$, $\hat{P}_{\gamma\gamma} = 0$). The J_β integrals are accordingly expressed as $J_\beta = J'_\beta + J''_\beta + \hat{J}_\beta$, where J'_β, J''_β, and $\hat{J}_\beta$ are defined in terms of the corresponding energy momentum tensors by expressions (15).

5.1 Configurational forces between two screw dislocations

To evaluate the configurational forces on the dislocation at O, exerted by the dislocation at A, the J_β integrals are evaluated along a small circle surrounding the center of the dislocation at O. The J'_β integrals vanish because the screw dislocation alone in an infinite medium does not exert any force on itself. The J''_β integrals also vanish, because the elastic stress field $''$ from the dislocation at A is non-singular within a small circle around the core of the dislocation at O. Thus, $J'_\beta = 0$, $J''_\beta = 0$, and J_β is again given by (16), with the components of the energy momentum tensor

$$\hat{P}_{11} = -\hat{P}_{22} = \frac{1}{\mu}\left(\sigma'_{32}\sigma''_{32} - \sigma'_{31}\sigma''_{31}\right), \quad \hat{P}_{12} = \hat{P}_{21} = -\frac{1}{\mu}\left(\sigma'_{31}\sigma''_{32} + \sigma'_{32}\sigma''_{31}\right). \tag{41}$$

The stress components due to screw dislocation in an infinite isotropic medium are well known [17,18]. Along a small circle of radius r around the dislocation at O, they are

$$\sigma'_{31} = -\frac{\mu b'_3}{2\pi}\,\frac{\sin\theta}{r}, \quad \sigma'_{32} = \frac{\mu b'_3}{2\pi}\,\frac{\cos\theta}{r}, \tag{42}$$

where b'_3 is the Burgers vector of the screw dislocation. The corresponding displacement field is $u'_3 = b'_3\theta/2\pi$. If the radius of the circle around dislocation at O is much smaller than the distance d from O to A, the stresses

along this circle due to dislocation b_3'' are nearly constant, and the substitution of (42) into (17), followed by integration, yields

$$J_1^O = \sigma_{23}'' b_3', \quad J_2^O = -\sigma_{13}'' b_3'. \tag{43}$$

These are the Peach–Koehler-type expressions for the force components on the screw dislocation at O. Since

$$\sigma_{13}'' \approx 0, \quad \sigma_{23}'' \approx -\frac{\mu b_3''}{2\pi d}, \tag{44}$$

the expressions for J_1^O and J_2^O integrals in (43) and, thus, the horizontal and vertical components of the force on the dislocation at O become

$$F_1^O = J_1^O = -\frac{\mu}{2\pi}\frac{b_3' b_3''}{d}, \quad F_2^O = J_2^O = 0. \tag{45}$$

6 Straight dislocations of mixed edged-screw type

Since there is no interaction between screw and edge components of two parallel dislocations, the components of the force on a straight dislocation at O due to a parallel dislocation at A are obtained by summing the contributions (27) and (45). This gives

$$F_1^O = -\frac{k}{d}\left[b_1' b_1'' + b_2' b_2'' + (1-\nu) b_3' b_3''\right], \quad F_2^O = \frac{k}{d}\left(b_1' b_2'' + b_1'' b_2'\right). \tag{46}$$

The corresponding glide and climb components of the force follow by substituting (46) into (29).

To illustrate the applications of the resulting formulas, consider four {111} slip planes of an FCC crystal, as shown in Fig. 6a. Two straight dislocations along $[1\bar{1}0]$ direction are shown in boldface, having their Burgers vectors $\mathbf{b}' = (a_0/2)[101]$ and $\mathbf{b}'' = (a_0/2)[0\bar{1}1]$, both of magnitude $a_0/\sqrt{2}$, where a_0 is the lattice parameter. The edge components of these dislocations are in the directions $[\bar{1}\bar{1}2]$ and $[112]$, with the magnitude $b_e' = b_e'' = (a_0/\sqrt{2})\sin 60^\circ = \sqrt{6}a_0/4$. The screw component of both dislocations is $(a_0/4)[1\bar{1}0]$, with the magnitude $b_s' = b_s'' = \sqrt{2}a_0/4$. The lattice section within the plane spanned by [110] and [001] directions is shown in Fig. 6b. The edge components of the considered two dislocations are also shown. The screw component of each dislocation is in the direction $[1\bar{1}0]$, which is orthogonal to the lattice section shown in Fig. 6b. The angle β between [110] and [112] directions is $\beta = 54.7^\circ$ ($\tan\beta = \sqrt{2}$). The objective is to determine the glide and climb components of the force on the dislocation at O as it glides along [112] direction from minus to plus infinity, assuming that the dislocation at A is pinned. An arbitrary configuration of two dislocations is shown in Fig. 7a. By geometry, $\varphi' = \beta + \gamma$ and $\varphi'' = \pi + \gamma - \beta$, where

$$\sin\gamma = \frac{c}{d}\sin\beta, \quad d^2 = a^2 + c^2 - 2ac\cos\beta, \quad (a = \sqrt{2}a_0), \tag{47}$$

and

$$\begin{aligned} b_1' &= b_e' \cos\varphi', \quad b_2' = b_e' \sin\varphi', \quad b_3' = b_s', \\ b_1'' &= b_e'' \cos\varphi'', \quad b_2'' = b_e'' \sin\varphi'', \quad b_3'' = b_s''. \end{aligned} \tag{48}$$

The variations of the glide and climb components of the force on the dislocation at O with the distance c are shown in Fig. 7b. They are determined by incorporating (46)–(48) into (29). The Poisson ratio is taken to be $\nu = 1/3$. For the considered geometry, as the distance between two dislocations increases, the climb component of the force decays to zero slower than the glide component of the force. The glide force vanishes at $c = 1.28a$ and $c = 2.71a$. The maximum negative glide force is $F_g^{\max} = -0.2167\,ka$, at $c = 0.6a$. The maximum positive glide force is $F_g^{\max} = 0.06\,ka$, at $c = 1.73a$. The maximum climb force is $F_c^{\max} = 0.1822\,ka$, at $c = 0.9a$. If $a = n \cdot \sqrt{2}a_0$ ($n > 1$), the forces are $(1/n)$ times the forces for $n = 1$.

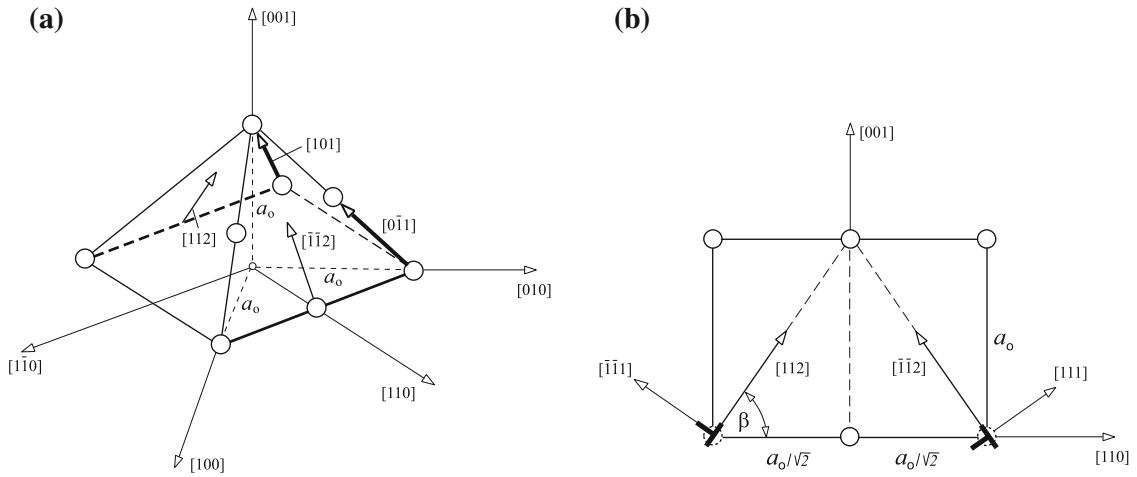

Fig. 6 **a** Four {111} slip planes of an FCC crystal. The Burgers vectors of two straight dislocations parallel to $[1\bar{1}0]$ direction are $(a_0/2)[101]$ and $(a_0/2)[0\bar{1}1]$. Their edge components are $(a_0/4)[112]$ and $(a_0/4)[\bar{1}\bar{1}2]$, respectively, while their screw component is $(a_0/4)[1\bar{1}0]$. **b** The mid-section of the lattice shown in part (**a**), spanned by [110] and [001] directions. The normal distance between the two slip planes is $d = (a_0/\sqrt{2})\sin\omega = a_0/\sqrt{3}$, where $\tan\omega = \sqrt{2}$

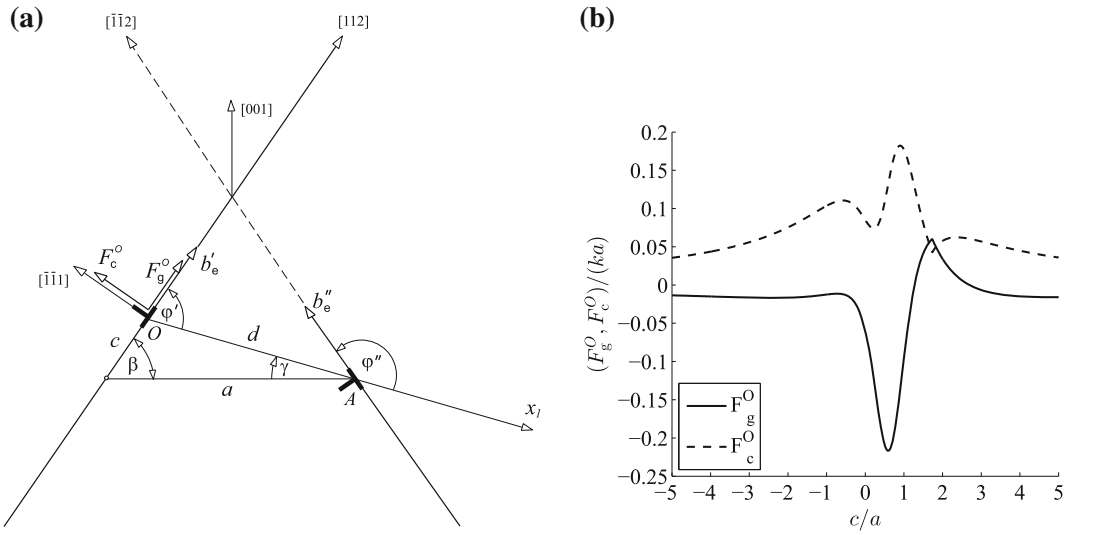

Fig. 7 **a** An arbitrary configuration of two dislocations, as the dislocation at O glides along its slip plane above the dislocation at A. Indicated are the glide and climb components of the force at O. **b** The variation of the glide and climb forces with the distance c. The forces are scaled by ka, where $k = \mu/[2\pi(1-\nu)]$ and $a = \sqrt{2}a_0$

7 Interactions among three dislocations

If there are more than two dislocations, the dislocation force on each dislocation is obtained by the superposition of its interactions with all other dislocations. For example, in the case of three screw dislocations along the same line (Fig. 8b), it can be readily shown that

$$J_1^O = -\frac{\mu}{2\pi}\left(\frac{b'_3 b''_3}{OA} + \frac{b'_3 b'''_3}{OB}\right), \quad J_1^A = \frac{\mu}{2\pi}\left(\frac{b''_3 b'_3}{OA} - \frac{b''_3 b'''_3}{AB}\right), \quad J_1^B = \frac{\mu}{2\pi}\left(\frac{b'''_3 b'_3}{OB} + \frac{b'''_3 b''_3}{AB}\right), \tag{49}$$

which satisfy $J_1^O + J_1^A + J_1^B = 0$. The third expression in (49) yields the expression for the force on the screw dislocation at the distance $OB = c$ from the center of a circular void of radius a (Fig. 9b), created by the displacement discontinuity b_3 from the center of the dislocation to infinity [19], by taking $OA = a^2/c$ and $b'_3 = b'''_3 = -b''_3 = b_3$. The magnitude of the force is $(a/c)^2$ times the magnitude of the force $(\mu b_3^2)/(2\pi d)$,

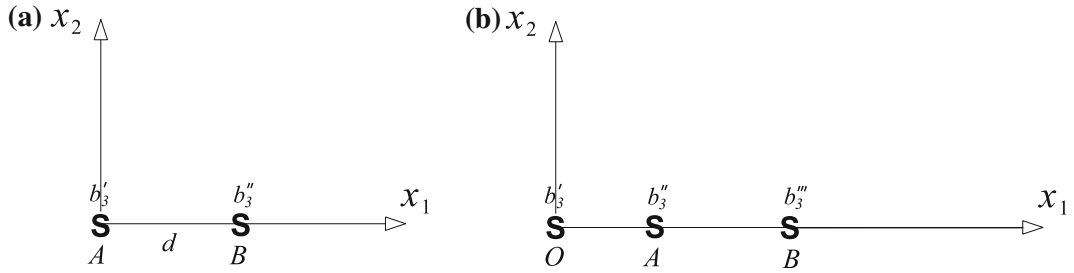

Fig. 8 **a** Two screw dislocations in an infinite medium at points A and B. The Burgers vectors of dislocations are b_3' and b_3''. **b** Three screw dislocations in an infinite medium at points O, A, and B. The Burgers vectors of dislocations are b_3', b_3'', and b_3'', respectively

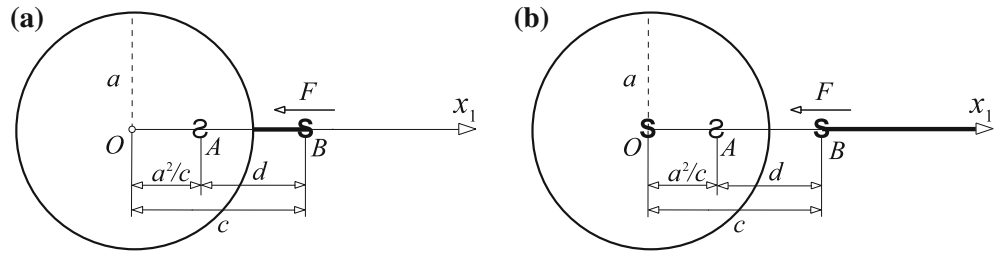

Fig. 9 **a** A screw dislocation at distance c from the center of a circular void of radius a, created by imposing the displacement discontinuity b_3 from the surface of the void to the center B of the dislocation. The dislocation is attracted to the surface of the void by the force $F = \mu b_3^2/(2\pi d)$. A negative image dislocation is placed at point A, at distance $d = c - a^2/c$ from the actual dislocation. **b** A screw dislocation at point B created by the displacement discontinuity b_3 from B to infinity. The dislocation force is $F = (a/c)^2 \mu b_3^2/(2\pi d)$. A positive image dislocation is placed at the center O, and a negative image dislocation at the conjugate point A

exerted by the surface of the void on the dislocation from Fig. 9a. The distance between the dislocation at B and its image dislocation at A in Fig. 9a is $d = AB = c - a^2/c$. The distinction between the two cases shown in Fig. 9 was first pointed out in [20] and further discussed in [21,22]. A recent study of the interaction between the eigenstrain inclusions and voids under plane strain and antiplane strain conditions has been reported in [23,24].

8 Interactions between screw dislocations and concentrated line forces

Similar analysis can be performed to evaluate the interaction between dislocations and other defects or singularities. For example, the force on a screw dislocation b_3 exerted by a concentrated line force f_3 (per unit length), at distance d from the dislocation (Fig. 10a), is obtained from (43) by substituting $\sigma_{13}'' = f_3/(2\pi d)$ and $\sigma_{23}'' = 0$, which gives $F_1^O = 0$ and $F_2^O = -f_3 b_3/(2\pi d)$. In the case of two concentrated forces f_3' and f_3'' (Fig. 10b), the J integrals around the forces are $J_1^A = -J_1^O = -f_3' f_3''/(2\pi\mu d)$ and $J_2^A = J_2^O = 0$, which are also the configurational forces on the line forces through O and A. While the configurational forces on two screw dislocations of the same sign are repelling, the configurational forces on two line forces of the same sign are attractive. This can be verified by an independent analysis, beginning with the energetic definition of $J_1^A = -\partial\Pi/\partial d$, where Π is the potential energy. The latter is equal to the strain energy minus the load potential,

$$\Pi = \frac{1}{2} f_3'(u_3'^O + u_3''^O) + \frac{1}{2} f_3''(u_3'^A + u_3''^A) - \left[f_3'(u_3'^O + u_3''^O) + f_3''(u_3'^A + u_3''^A) \right], \tag{50}$$

where $u_3'^O$ is the (singular) displacement at O due to f_3' and $u_3''^O$ is the (non-singular) displacement at O due to f_3'' at A. Similar interpretations apply to $u_3''^A$ and $u_3'^A$. In view of the reciprocity relation of linear elasticity $f_3' u_3''^O = f_3'' u_3'^A$, the expression (50) reduces to

$$\Pi = -\frac{1}{2} \left(f_3' u_3'^O + f_3'' u_3''^A \right) - f_3' u_3''^O. \tag{51}$$

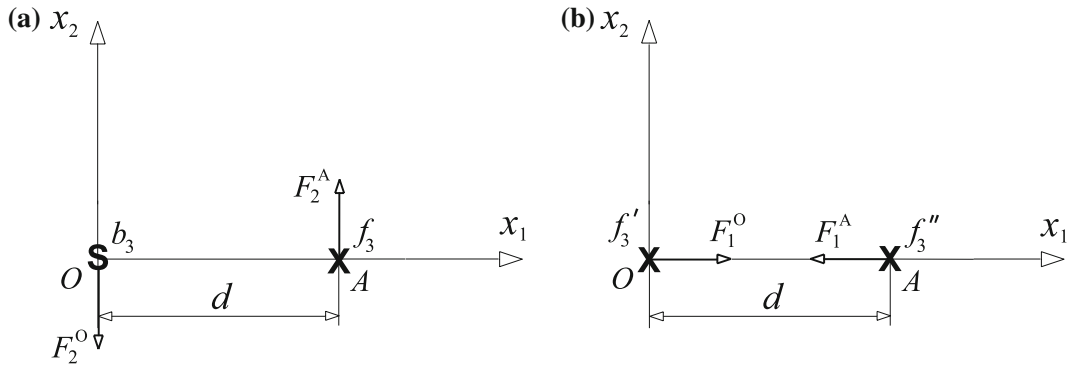

Fig. 10 **a** A concentrated line force f_3 at the distance d from the screw dislocation b_3. Their interaction forces (of the same magnitude) are F_2^O and F_2^A. **b** Attractive configurational forces F_1^O and F_1^A (of the same magnitude) between two parallel line forces f_3' and f_3'' of the same sign

Furthermore, since

$$u_3''^{\,O} = -\frac{f_3''}{2\pi\mu}\ln\frac{d}{R}, \tag{52}$$

where R is an arbitrary constant length, the potential energy (51) becomes

$$\Pi = -\frac{1}{2}\left(f_3' u_3'^{\,O} + f_3'' u_3''^{\,A}\right) + \frac{f_3' f_3''}{2\pi\mu}\ln\frac{d}{R}. \tag{53}$$

The first two terms on the right-hand side (although singular)[4] are independent of d, so that

$$J_1^A = -\frac{\partial\Pi}{\partial d} = -\frac{f_3' f_3''}{2\pi\mu}\frac{1}{d}. \tag{54}$$

Thus, if two line forces are of the same sign, the configurational forces on them are attractive, because the potential energy is increased by the increase in the distance between such forces. For instance, the free surface of a half-space exerts an attractive force on a nearby line force, because the image force of the same sign is placed in an infinite medium at the mirror position across the surface to make this surface traction free.

If two parallel line forces (f_3' and f_3'') are acting along the surface of a half-space (Fig. 11), at a distance d from each other, they attract each other with the force $f_3' f_3''/(\pi\mu d)$, provided that they are in the same direction. The repulsion of the same magnitude occurs if they are in the opposite directions. The results follows directly from the previous analysis of the line forces in an infinite medium by recalling that the nonvanishing stress component (in polar coordinates) due to the line force (f_3) along the surface of a half-space is $\sigma_{3r} = -f_3/(\pi r)$, with the coordinate origin at the location of the force [25].

In the case of plane strain, the use of line forces on the surface of a half-space has been used to model a step on vicinal or corrugated surfaces [26–28]. There has also been a considerable activity devoted to edge contact forces which appear in the framework of second gradient media [29–32]. Energetic interaction of such forces may be a worthwhile topic of further investigation.

9 Conclusions and discussion

The expressions for the glide and climb components of the force exerted on a straight dislocation in an infinite isotropic medium by another straight dislocation are derived by evaluating the plane or antiplane strain versions of the J integrals. To circumvent tedious evaluation of the integrals using the total stress and displacement fields,

[4] If ρ is a radius of small circle around each force, then the first term can be written as

$$-\frac{1}{2}\left(f_3' u_3'^{\,O} + f_3'' u_3''^{\,A}\right) = \frac{1}{4\pi}\left(f'^2 + f''^2\right)\ln\frac{\rho}{R},$$

in the limit as $\rho \to 0$. In the derivation, it is recalled that $\sigma_{3r} = -f_3/(2\pi r)$ and $u_3 = -(f_3/2\pi\mu)\ln(r/R)$.

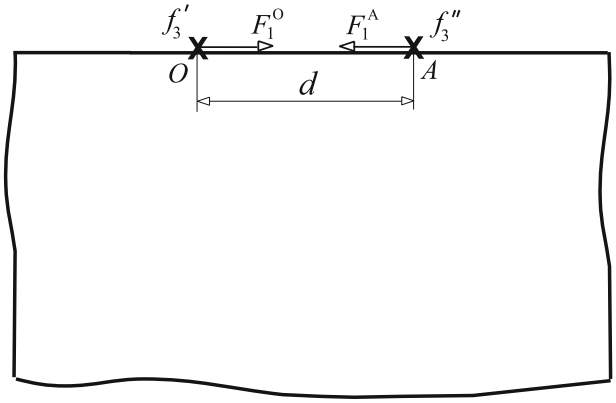

Fig. 11 Two parallel line forces f_3' and f_3'' along the surface of a half-space at the distance d from each other. Their interaction forces F_1^0 and F_1^A (attractive if f_3' and f_3'' are in the same direction) are defined such that the change in the potential energy of the system, associated with the increase in the distance δd, is $\delta\Pi = F_1^A \delta d$

these are expressed as the sums of the elastic fields from each dislocation, which enabled the decomposition of the energy momentum tensor into three parts. Only one part of them, involving mixed products from the two dislocation fields, makes a nonvanishing contribution to the J integrals and the corresponding dislocation forces. Three examples are used to illustrate the procedure, with the dislocations on parallel or intersecting slip planes. The interaction between dislocations and a nearby circular void, as well as between parallel line forces in an infinite or semi-infinite medium under antiplane strain conditions are also discussed.

Although the analysis in this paper was concerned with the evaluation of the configurational forces among defects by the evaluation of the J integrals, the utilized decomposition of the energy momentum tensor also facilitates the evaluation of the M integrals. For example, the M integral along a small circle around the screw dislocation at A (Fig. 8a) is

$$M_A^A = \oint P'_{\alpha\beta} n_\alpha x_\beta \, \mathrm{d}l = \frac{\mu b_3'^2}{4\pi}, \tag{55}$$

because the contributions from $P''_{\alpha\beta}$ and $\hat{P}_{\alpha\beta}$ both vanish. In (55), the superscript A refers to M integral around dislocation at A, while the subscript A indicates that the coordinate origin used in evaluating the M integral was placed at A. As elaborated upon in [33,34], the M integral can be conveniently used to evaluate the J integral indirectly. The M integral along a closed contour consisting of small circles around the center of dislocations at A and B, and a remote circle of radius $R \to \infty$, surrounding both dislocations, must vanish, so that $M_A^A + M_A^B - M_A^R = 0$. Here, M_A^R denotes the M integral along a closed contour of large radius R. Furthermore, from the well-known relationship between the M integrals evaluated with respect to two coordinate origins [35], one can write for the M integral around the dislocation at B, $M_A^B = M_B^B + d \cdot J_1^B$, so that $J_1^B = (M_A^R - M_A^A - M_B^B)/d$. Since

$$M_B^B = \frac{\mu b_3''^2}{4\pi}, \quad M_A^R = \frac{\mu (b_3' + b_3'')^2}{4\pi}, \tag{56}$$

there follows

$$J_1^B = \frac{\mu b_3' b_3''}{2\pi d}. \tag{57}$$

As pointed out in Sect. 7, this expression delivers the expression for the force exerted by the surface of a circular void on the dislocation emitted from that surface by taking $d = c - a^2/c$ and $b_3'' = -b_3' = b_3$, where a is the radius of the void and c is the distance between the dislocation and the center of the void (Fig. 9a).

The considerations in this paper were based on the Volterra dislocation model and linear elasticity. The dislocations were assumed to be fully formed and therefore sufficiently away from each other or from other defects, perhaps by at least two lengths of their Burgers vector. Otherwise, incomplete dislocations, dominated by their heavily distorted cores, would be present, which requires another type of analysis, such as that based on the Peierls dislocation model [36,37]. The energy momentum tensor has also been used for different problems

in the range of finite elastic and inelastic deformations. The representative references include, inter alia, [38–40]. The energy momentum and dual energy momentum tensors in problems of micropolar elasticity, with and without body forces or body couples, were recently discussed in [41].

Acknowledgments Research support from the Montenegrin Academy of Sciences and Arts is gratefully acknowledged. I also thank anonymous reviewers for their helpful comments and suggestions.

References

1. Eshelby, J.D.: The force on an elastic singularity. Philos. Trans. R. Soc. A **244**, 87–112 (1951)
2. Eshelby, J.D.: The continuum theory of lattice defects. Solid State Phys. **3**, 79–144 (1956)
3. Cherepanov, G.P.: The propagation of cracks in a continuous medium. J. Appl. Math. Mech. **31**, 503–512 (1967)
4. Rice, J.R.: A path independent integral and approximate analysis of strain concentration by notches and cracks. J. Appl. Mech. **38**, 379–386 (1968)
5. Günther, W.: Über einige Randintegrale der Elastomechanik. Abh. Braunschw. Wiss. Ges **14**, 53–72 (1962)
6. Knowles, J.K., Sternberg, E.: On a class of conservation laws in linearized and finite elastostatics. Arch. Ration. Mech. Anal. **44**, 187–211 (1972)
7. Budiansky, B., Rice, J.R.: Conservation laws and energy-release rates. J. Appl. Mech. **40**, 201–203 (1973)
8. Maugin, G.A.: Material forces: concepts and applications. Appl. Mech. Rev. **48**, 247–285 (1995)
9. Gurtin, M.E.: Configurational Forces as Basic Concepts of Continuum Mechanics. Springer, New York (2000)
10. Kienzler, R., Herrmann, G.: Mechanics in Material Space. Springer, Berlin (2001)
11. Maugin, G.A.: Configurational Forces: Thermomechanics, Physics, Mathematics and Numerics. CRC Press/Taylor & Francis, Boca Raton (2011)
12. Peach, M., Koehler, J.C.: The forces exerted on dislocations and the stress fields produced by them. Phys. Rev. Lett. **80**, 436–439 (1950)
13. Lubarda, V.A., Blume, J.A., Needleman, A.: An analysis of equilibrium dislocation distributions. Acta Metall. Mater. **41**, 625–642 (1993)
14. Lubarda, V.A.: On the elastic strain energy representation of a dislocated body and dislocation equilibrium conditions. J. Elast. **32**, 19–35 (1993)
15. Lubarda, V.A.: Dislocation equilibrium conditions revisited. Int. J. Solids Struct. **43**, 3444–3458 (2006)
16. Müller, W.H., Kemmer, G.: Applications of the concept of J-integrals for calculation of generalized forces. Acta Mech. **129**, 1–12 (1998)
17. Hirth, J.P., Lothe, J.: Theory of Dislocations. 2nd edn. Wiley, New York (1982)
18. Nabarro, F.R.N.: Theory of Crystal Dislocations. Dover Books on Physics and Chemistry (1987)
19. Friedel, J.: Dislocations. Pergamon Press, Oxford (1964)
20. Lubarda, V.A.: On the non-uniqueness of solution for screw dislocations in multiply connected regions. J. Elast. **52**, 289–292 (1999)
21. Lubarda, V.A.: Image force on a straight dislocation emitted from a circular void. Int. J. Solids Struct. **48**, 648–660 (2011)
22. Lubarda, V.A.: Emission of dislocations from nanovoids under combined loading. Int. J. Plast. **27**, 181–200 (2011)
23. Lubarda, V.A.: Interaction between a circular inclusion and a circular void under plane strain conditions. J. Mech. Mater. Struct. (in press) (2015)
24. Lubarda, V.A.: Circular inclusion near a circular void: determination of elastic antiplane shear fields and configurational forces. Acta Mech. **226**, 643–664 (2015)
25. Barber, J.R.: Elasticity, 3rd rev. ed. Springer, Dordrecht (2010)
26. Müller, P., Saúl, A.: Elastic effects on surface physics. Surf. Sci. Rep. **54**, 157–258 (2004)
27. Wang, Y., Weissmüller, J., Duan, H.L.: Mechanics of corrugated surfaces. J. Mech. Phys. Solids **58**, 1552–1566 (2010)
28. Li, W.N., Duan, H.L., Albe, K., Weissmüller, J.: Line stress of step edges at crystal surfaces. Surf. Sci. **605**, 947–957 (2011)
29. Germain, P.: La méthode des puissances virtuelles en mécanique des milieux continus. Première partie: Théorie du second gradient. J. de Mécanique **12**, 235–274 (1973)
30. dell'Isola, F., Seppecher, P.: Edge contact forces and quasi-balanced power. Meccanica **32**, 33–52 (1997)
31. Podio-Guidugli, P., Vianello, M.: Hypertractions and hyperstresses convey the same mechanical information. Cont. Mech. Thermodyn. **22**, 163–176 (2010)
32. Javili, A., dell'Isola, F., Steinmann, P.: Geometrically nonlinear higher-gradient elasticity with energetic boundaries. J. Mech. Phys. Solids **61**, 2381–2401 (2013)
33. Freund, L.B.: Stress intensity factor calculations based on a conservation integral. Int. J. Solids Struct. **14**, 241–250 (1978)
34. Rice, J.R.: Conserved integrals and energetic forces. In: Bilby, B.A., Miller, K.J., Willis, J.R. (eds.) Fundamentals of Deformation and Fracture, pp. 33–56. Cambridge University Press, Cambridge (1985)
35. Asaro, R.J., Lubarda, V.A.: Mechanics of Solids and Materials. Cambridge University Press, Cambridge (2006)
36. Lubarda, V.A., Markenscoff, X.: A variable core model and the Peierls stress for the mixed (screw-edge) dislocation. Appl. Phys. Lett. **89**, Art. No. 151923 (2006)
37. Lubarda, V.A., Markenscoff, X.: Configurational force on a lattice dislocation and the Peierls stress. Arch. Appl. Mech. **77**, 147–154 (2007)
38. Eshelby, J.D.: The elastic energy momentum tensor. J. Elast. **5**, 321–335 (1975)
39. Epstein, M., Maugin, G.: The energy-momentum tensor and material uniformity in finite elasticity. Acta Mech. **83**, 127–133 (1990)

40. Gupta, A., Steigmann, D.J., Stölken, J.S.: On the evolution of plasticity and incompatibility. Math. Mech. Solids **12**, 583–610 (2007)
41. Lubarda, V.A.: Dual Eshelby stress tensors and related integrals in micropolar elasticity with body forces and couples. Eur. J. Mech. A/Solids **36**, 9–17 (2012)